Optimizing Control of an Experimental Simulated Moving Bed Unit

Gültekin Erdem and Manfred Morari
ETH Zurich, Automatic Control Laboratory, Zurich, Switzerland

Mohammad Amanullah and Marco Mazzotti
ETH Zurich, Institute of Process Engineering, Zurich, Switzerland

Massimo Morbidelli
ETH Zurich, Institute for Chemical and Bio-Engineering, Zurich, Switzerland

DOI 10.1002/aic.10802
Published online March 1, 2006 in Wiley InterScience (www.interscience.wiley.com).

Simulated moving bed (SMB) chromatography has become a key separation technology in the areas of pharmaceutical and biotechnology industry thanks to its high productivity and short process development times. Today, modeling, design, and optimization of the SMB process are regarded to be well established. On the other hand, long term robust/optimized operation of the process is still an open issue. The common practice is to operate the SMB units under suboptimal operating conditions in order to gain the necessary robustness. The operating parameters are tuned manually by experienced operators in order to maintain the product specifications in the long term. Therefore, as SMB applications spread, the SMB process control problem becomes increasingly important. Recently, we have proposed an on-line optimization based SMB control scheme that allows exploiting the full economic potential of the SMB technology on the basis of minimal information. This work addresses the experimental implementation of the developed control concept on an eight-column four-section laboratory SMB unit that is used to separate the binary mixture of nucleosides uridine and guanosine. The performance of the SMB control scheme is demonstrated via several experimental controlled SMB runs that are designed to challenge the robust performance of the controller. The reported results aim to demonstrate that the controller is able to deliver the products with the specified purities and to optimize the process performance despite uncertainties in the system behavior and disturbances taking place during the operation. © 2006 American Institute of Chemical Engineers *AIChE J,* 52: 1481–1494, 2006
Keywords: simulated moving bed chromatography, online optimization, optimizing control, repetitive model predictive control

Introduction

Stricter regulations from regulatory agencies (FDA, EMEA) and growing environmental concerns force pharmaceutical, agrochemical, and food industries to need even purer products. Moreover, the development of purer products with improved biological/pharmaceutical activity allows the extension of existing patents, providing the companies with a longer time for their exploitation.

Preparative chromatography has been playing an important role as a separation and purification process in these industries wherever classical techniques such as distillation are not fea-

Correspondence concerning this article should be addressed to M. Morari at morari@control.ee.ethz.ch.

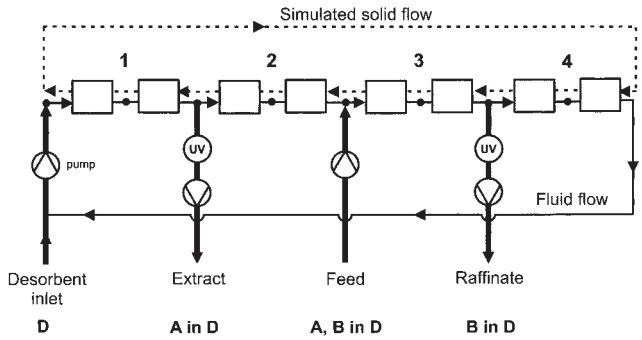

Figure 1. Scheme of a simulated moving bed (SMB) unit including UV detectors for on-line concentration measurements in extract and raffinate.

sible. A remarkable breakthrough has been achieved by the development of continuous simulated moving bed (SMB) chromatography for fine chemical separations, which allows achieving significant advantages over batch chromatography in terms of process performance, namely, a reduced desorbent consumption and a higher productivity per unit mass of the stationary phase. Moreover, SMBs can be operated using the same method (same stationary phase and mobile phase) adopted for small-scale preparative batch processes. This constitutes the success of the SMB technology as a tool for speeding up the development process of new fine chemical or pharmaceutical products, which represents a major challenge faced by pharmaceutical companies today.

The SMB process involves a countercurrent contact between the fluid phase carrying the components to be separated and the stationary phase, which is accomplished in a simulated fashion. In fact, an SMB unit comprises a number of chromatographic columns, separated by ports where inlet and outlet streams can be fed or collected (see Figure 1). The countercurrent movement of the solid phase is simulated by periodically and synchronously shifting the feed and withdrawal ports of the unit in the same direction as the mobile phase flow. A standard SMB unit has four external streams: the feed mixture to be separated; the desorbent, that is, the eluent or the mixture of eluents constituting the mobile phase; the extract stream enriched in the more retained species; and the raffinate stream enriched in the less retained species.[1] These streams divide the unit in four sections (section I between the desorbent inlet and the extract port; section II between the latter and the feed inlet; section III between this and the raffinate outlet; and section IV between the raffinate port and the desorbent inlet); each section plays a specific role in the process. The separation is performed in sections II and III, where the less retained species must be desorbed and carried by the mobile phase towards the raffinate outlet. On the other hand, the more retained species must be adsorbed by the stationary phase and carried towards the extract port due to the simulated solid movement. In section I, the stationary phase is regenerated by the fresh mobile phase stream, which desorbs the more retained species; and finally, in section IV, the mobile phase is purified through adsorption of the less retained species. In such a way. both the stationary and the mobile phase can be recycled to sections IV and I, respectively.

As the number of production scale SMB applications has grown, research has focused on the improvement of the economical aspects of the process, thus showing that the possible gain from optimization is significant.[2,3] Unfortunately, only a small part of this gain can be utilized in practice, and the full economic potential of the SMB process is still to be exploited. This has two main reasons. First, precise characterization of the system, such as measurement of the isotherm parameters and single column properties, is rather difficult. Moreover, the system undergoes changes during operation, for instance due to chemical and mechanical aging of the stationary phase. Obviously, the effectiveness of the optimization tools is limited by the accuracy of the available physical data. Second, SMB units are highly sensitive to uncertainties and disturbances, such as temperature deviations, pump inaccuracy, feed and solvent composition changes, and so on, when they are operated close to their optimum operating conditions.[4] As a consequence, SMB units are operated at a certain distance from their optimal operating conditions in order to obtain sufficient robustness and guarantee product quality. In general, suboptimal operating conditions of SMB units are tuned manually by experienced operators in order to fulfill the product specifications. Available short-cut design tools, such as triangle theory,[4] provide explicit rules and ease this task for the operators.

The production scale application of SMB technology poses the challenge of guaranteeing long-term product quality and robust-optimized operation. Development and implementation of SMB control schemes is the natural solution to the above problems. Hence, as the applications of SMB spreads, SMB process control becomes a major issue in the scientific literature and in the community of industrial practitioners. Note that the SMB process never reaches a steady-state with constant profiles of the process variables. Its stationary regime is a cyclic one in which the process variables undergo a transient, i.e., the concentration profiles in the SMB propagate in the direction of the fluid flow and are shifted backwards with respect to the inlet/outlet ports with each inlet/outlet port switch. Therefore, the mixed continuous/discrete and nonsteady-state nature of the SMB process poses a challenging control problem.

Contrary to a significant number of works addressing its modeling, simulation, and optimization, there are only a few works on the control of SMB processes. In this article, we first provide an overview of the SMB control approaches reported in the literature; and then we address the experimental verification of our own SMB control concept, whose features are highlighted. To this aim, the control scheme is implemented on a lab-scale, eight-column, four-section SMB unit used for the high purity separation of the nucleosides uridine and guanosine, which are retained on the stationary phase following a linear adsorption isotherm. The effectiveness of the control scheme is verified by several experimental test runs.

The article is organized as follows: After the literature overview in the second section, the SMB control scheme is introduced in the third section. Because its detailed description is available elsewhere,[5,6] only a short description is provided here. The fourth and fifth sections are devoted to the experimental implementation of the control concept and report several experimental test runs that are designed to challenge the control scheme. Finally, conclusions are drawn in the last section.

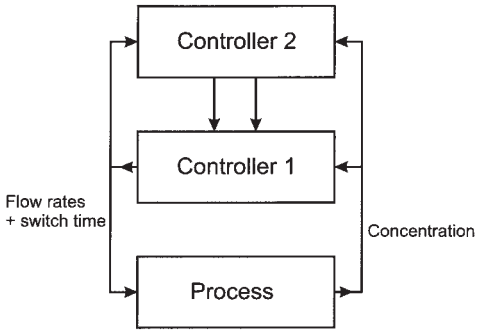

Figure 2. Two layer control strategies.

Background

State of research on SMB control

The development of an SMB control concept has been undertaken by a number of research groups, which have proposed model based control schemes that can be classified into two main categories. The control strategies within the first category identify the optimum of the process by off-line optimization techniques, that is, based on detailed SMB models or short-cut methods, by assuming that sufficiently accurate physical data of the system are available a priori. The controllers are designed to operate the plant at optimal operating conditions despite disturbances. They either make use of a true moving bed (TMB) model to approximate the SMB dynamics or develop the model in such a way that the mixed continuous/discrete and non-steady-state nature of the SMB process is hidden from the controller. In this way, the difficulties connected with the hybrid nature of the process are overcome.

Kloppenburg and Gilles[7] proposed an automatic control scheme for an SMB unit applied to the separation of C_8 aromatics. The optimal operating conditions of the SMB unit are determined off-line using a TMB model. The same type of model is used to estimate and control the SMB behavior using feedback information only at the middle of the switching intervals under the assumption that a TMB model represents the SMB dynamics well enough for systems with a high number of columns, such as 24 columns. The controller is designed using the principle of asymptotically exact input/output linearization. Song et al.[8] obtained an input/output data-based prediction model by using subspace identification. The obtained model was then used to design a linear model predictive controller (MPC) to keep the process on the pre-calculated optimal concentration trajectories despite the disturbances.

Schramm et al.[9] introduced a concept that makes use of nonlinear wave propagation phenomena. Relationships between the front movements and the net flow rate ratios in every section of the equivalent TMB process are derived on the basis of the nonlinear wave theory, which are then used to calculate the optimal operating conditions. Two PI controllers are used to adjust the movements of the wave fronts in the two central sections and to control the product purities. The controller delivers the maximum feed throughput provided that the isotherm parameters are correct and the regeneration of the solid and liquid phases is guaranteed. The control strategies in this first category calculate the optimal operating trajectories off-line and then define the control problem as a tracking or regulation problem; therefore, they require accurate physical data. This is one of the major intrinsic difficulties for the optimal operation of SMB units. Moreover, predefined optimal trajectories are hardly applicable for the SMB process because such trajectories depend on operating parameters, such as feed concentration/composition, and the physical parameters of the system, which are subject to change. Therefore, frequent re-characterization and off-line re-optimization of the process are presumably not avoidable.

The SMB control approaches within the second category have tried to overcome these problems by introducing a two layer control scheme. On one level the process parameters, that is, the physical properties characterizing the system behavior, are estimated and/or the optimal operating trajectories of the process are calculated, that is, corresponding to Controller 2 in Figure 2. On the other level, the controllers are designed either to have the process follow the calculated optimal trajectories or to optimize the operating conditions on-line on the basis of estimated physical parameters, that is, corresponding to Controller 1 in Figure 2. Table 1 provides a comparison of SMB control approaches available in the literature. Note that the control strategies that do not have a higher level component, namely, Controller 2 in Figure 2 and in Table 1, are considered to be in the first category.

Klatt et al.[10,11] introduced the first two layer control scheme. On the upper level, the optimal operating trajectory of the process is calculated by off-line optimization, that is, based on detailed SMB models. On the lower level, local SISO internal model controllers (IMC), that is, based upon linear ARX type identification local models, are designed to keep the process on the optimal trajectory, that is, to maintain the position of the internal profiles, despite the disturbances. They used a sampling interval equal to one switching period to avoid the difficulties introduced by the switching mechanism. Changes in the operating parameters necessitate estimation of the system parameters on the basis of on-line measurements, off-line re-

Table 1. Comparison of Different SMB Control Approaches Proposed by Different Research Groups

Approach	Kloppenburg et al.[7]	Song et al.[8]	Schramm et al.[9]	Klatt et al.[10,11]	Wang et al.[12,13]	Toumi et al.[14,15]
Controller 1	I/O Linearization	Linear MPC	PI	IMC based on local models	Linear MPC	Nonlinear MPC
Controller 2	None	None	None	Optimization of operating conditions + Physical parameter estimation	Neural network adaptation	Physical parameter estimation
Controller 2 output	None	None	None	Physical parameters + Optimal trajectory + Local models	Linear model parameters	Physical parameters
Controller 2 input	None	None	None	Concentration + Flow rates	Concentration + Flow rates	Concentration + Flow rates

optimization of the process to update the optimal trajectory, and re-synthesis of the local controllers based on the updated optimal trajectory on the upper level of the control architecture.

Since the control scheme with local linear models was found to be insufficient to maintain the position of the internal profiles under nonlinear chromatographic conditions, the same research group has also investigated the use of neural network-based identification and model predictive control for SMBs.[12,13] In that case, linear models are obtained by successively linearizing identified multi-layer neural network (NN) models. These models are used within a standard linear MPC algorithm to keep the adsorption and desorption fronts at their pre-calculated optimal positions. Like the other control approaches, the switching time is set equal to the discrete sampling time of the system to hide the hybrid dynamics of the process to the controller.

Finally, Toumi and Engell[14,15] have proposed a nonlinear MPC scheme that is applied to a three-section, six-column reactive SMB (SMBR) unit (with 1–2-3 configuration). SMBR is used to combine the continuous chromatographic separation with the enzymatic biochemical conversion of glucose to fructose, thus overcoming the equilibrium limitations and improving the process performance. Fructose is the only product; hence, the SMBR has only one product outlet. Actually, the proposed control scheme can be considered as the logical continuation of the ones presented previously by the same research group. They started with a relatively simple scheme based on local ARX type identification models,[10,11] then took a further step in terms of computational complexity and used NN models to represent the SMB dynamics. The computational difficulties in nonlinear MPC are avoided by linearizing the NN models.[12,13] Finally, in this scheme, they make use of a nonlinear rigorous process model for the on-line optimization of the process. Because the solution of a non-convex optimization problem may need formidable computational effort and time, they modified the control problem such that the emphasis is on the calculation of a suboptimal but feasible solution under real time constraints, that is, the sampling time for the controller was defined as one switch period, which was around 17 minutes for the considered SMB application. As also stated by the authors, accurate values of the model parameters are needed for the use of the process model for optimization and control. Therefore, the necessary physical parameters are obtained beforehand by mathematical fitting of simulation runs to experimental data using the model parameters as optimization variables, and then adapted on-line with a similar algorithm by using available measurements. The initially estimated parameters are used to calculate the optimal startup operating conditions off-line. The authors report an experimental run with the proposed controller where they specify the desired product purity as 55%. The desorbent flow rate, recycle flow rate, and switching period, modified only from cycle to cycle, were used as the manipulated variables. The task of the controller was to minimize the desorbent consumption for a pre-defined feed flow rate. The controller managed to keep the product purity above the desired level. On the other hand, because of enzyme concentration changes from column to column, which cause variations in single column characteristics, and temperature gradient over the columns, the product purity fluctuated above the specified level.

At the heart of all these control strategies is the availability and/or the on-line estimation of precise physical data of the system. The precise off-line characterization of the system is a challenging task in itself. Clearly, the on-line estimation of the system parameters is an even more difficult endeavor. Moreover, they rely on the accuracy of the rigorous SMB models for both the off-line calculation of the optimal operating trajectories and the on-line optimization of the process. Unfortunately, it is not easy to incorporate precisely the effect of system uncertainties, such as uneven dead volumes in different sections of the SMB unit and differences in the column-to-column performance that always exist in practice, on the optimal operating conditions or trajectories. This becomes even more difficult if the periodicity of the process is defined over successive switches because the real period of the SMB process is one full cycle, that is, number of switches equal to the number of columns, not a single switch, due to the above mentioned nonidealities. In conclusion, the critical issue in SMB control is the robust performance of the control scheme under model and parameter uncertainties.

State of our research

Recently, Lee et al.[16] formulated a new model predictive control (MPC) method, so-called repetitive model predictive control (RMPC), and proposed it for the control of periodic processes such as SMB chromatography.[17] Subsequently, we have proposed an on-line optimization based SMB control scheme that makes use of RMPC.[5]

The effectiveness of this control approach has been demonstrated through extensive simulations in different cases (model/plant mismatch, disturbances), and for different linear and nonlinear adsorption isotherms.[18-20] The developed SMB control scheme has several noteworthy features:

- The control problem is formulated as a general constrained dynamic optimization problem that is solved on-line; therefore, all product specifications and hardware limitations can be considered as constraints in the optimization problem. Moreover, it gives the flexibility to choose the economic objective of the operation freely, such as minimization of the desorbent consumption, maximization of the productivity, or a combination thereof.
- The control scheme does not require any a priori knowledge of optimal operating conditions or initially calculated optimal trajectories.
- The control scheme requires only a minimal number of physical parameters to be determined off-line once before the operation.
- The knowledge of the adsorption behavior of the mixture under linear chromatographic conditions, that is, characterized by linear adsorption isotherm parameters, and of the average void fraction of the columns in the SMB unit is sufficient even if the SMB unit operates under nonlinear chromatographic conditions. This significantly reduces the amount of information necessary to design, optimize, operate, and control a new SMB separation.[6,18,20]
- The controller can handle the effects of extra-column dead volume differences among the sections and of column-to-column variations without any extra modeling effort.

Recently, we have reported the experimental implementation details of the controller together with the first controlled SMB separation results.[21] Here, the robust performance of the con-

trol scheme is thoroughly examined by several experimental SMB runs that are also designed to demonstrate some of the above features.

On-line optimization based SMB control scheme

Model predictive control has been widely adopted in industry as an effective control technique to address multivariable constrained control problems.[22] The fundamental idea of MPC is to employ an explicit model of the process in order to predict its future behavior over a time interval, a so-called prediction horizon. The control problem is defined such that the performance of the process is optimized on-line over the prediction horizon. In the optimization problem, the objective function quantifies the process objectives and the process and/or hardware restrictions are imposed as constraints. The on-line solution of the optimization problem yields the optimal control inputs for a chosen future time window, the so-called control horizon, which are then implemented according to a receding horizon strategy: the first element of the calculated optimal control sequence, that is, corresponding to the current time t, is implemented and the remaining elements are discarded. As new measurements are collected from the plant, a new optimization problem is solved at time $t + 1$.

In principle, any type of model can be used to represent the dynamics of the process to be controlled. However, obtaining a model of the process for control purposes has been one of the bottlenecks in SMB control. An SMB model representing the key characteristics of the process, that is, its hybrid (continuous/discrete) and periodic dynamics, is desirable. Therefore, at first, employing rigorous dynamic models of SMB seems attractive. However, on-line optimization of the process on the basis of detailed SMB models requires significant modeling and computational effort[14] and leads to nonlinear programming problems introducing complexities and computational difficulties.[22] Consequently, there is a clear need to identify the proper trade-off between level of detail and level of complexity of the model and the resulting computational effort. Most research groups involved in SMB control have tried to address this problem by obtaining black-box models, which are designed in a way that the hybrid and periodic nature of the process is hidden to the controller, such as by using a sampling interval equal to the switching period.

In this work, we obtain a linear time-varying (LTV) SMB model via linearization of a detailed equilibrium dispersive (ED) SMB model.[5] The LTV SMB model is designed such that the manipulated variables are the internal flow rates in the four sections of the unit, that is, $Q_I, \ldots, Q_{IV,}$ and the measured-output variables are the concentration levels in the two outlet streams, i.e., c_A^R, c_B^R, c_A^E, c_B^E.

Since the SMB process has a time-varying cyclic steady-state dynamics, we have defined N time instances ($N = 64$ in this case) within the duration of a cycle, and then obtained N different internal profiles, that is, each corresponding to one of the N sampling times, by simulating the process with the detailed ED model of the SMB. The nonlinear ED SMB model is then linearized at each sampling time using the corresponding cyclic steady-state concentration values and the flow rates in the four sections. This procedure leads to a linear time-varying state-space SMB model that has the following structure:

$$x_k(n+1) = A(n)x_k(n) + B(n)u_k(n)$$
$$x \in \mathbf{R}^{n_{eq}},\ u \in \mathbf{R}^{n_u},\ y \in \mathbf{R}^{n_y}$$
$$y_k(n) = C(n)x_k(n) \quad \text{for} \quad n = 0, \ldots, N-1 \qquad (1)$$

In the equation above, k is the cycle index and n is the time index running within the cycle index; x and u are the state and input vectors comprising the internal concentration values along the unit and the internal flow rates, respectively; n_{eq}, n_y, and n_u indicate the dimension of the system and the number of process inputs and outputs, respectively. The concentration levels at both outlets, that is, $c_A^R(n)$, $c_B^R(n)$, $c_A^E(n)$, $c_B^E(n)$, constitute the output vector y. All variables are defined in terms of deviation variables. For instance, the manipulated variable vector is defined as $u(n) = \mathbf{Q}(n) - \mathbf{Q}^{ref}(n)$, where $\mathrm{Q}(n) = [Q_I(n)\ Q_{II}(n)\ Q_{III}(n)\ Q_{IV}(n)]^{\mathrm{T}}$ and $\mathbf{Q}^{ref}(n)$ is the vector comprising the flow rates that are used for linearization.

For the transition from one cycle to the next we impose:

$$x_{k+1}(0) = x_k(N) \qquad (2)$$

This implies that the space composition profiles at the end of cycle k are used as initial conditions for the next cycle $k + 1$. The resulting LTV state-space model captures both the time dependent cyclic steady-state and the hybrid nature of the process explicitly through the time-varying state-space matrices (Eq. 1) and the cycle-to-cycle transition operator (Eq. 2).

The order of the LTV model is reduced by the balanced model reduction technique,[5] and the reduced model constitutes the basis for the formulation of the control problem along the lines of RMPC. The RMPC formulation exploits the periodic nature of repetitive processes and combines the advantages of repetitive control and MPC.[16] Note that, since the SMB process has a periodic nature, possible model prediction errors and the effects of periodwise constant disturbances are likely to repeat from cycle to cycle. Therefore, in the framework of RMPC, these are lumped into a linear error term on the plant output and estimated by using the available measurements. The estimated error is transferred to the future cycles as part of the states of the system and then used to correct for the possible future model prediction errors. In our case, a periodic time-varying Kalman filter serves to combine the measurement information and the model estimation in an optimal sense in order to correct the model errors recursively (see Figure 3).[23] We refer to earlier literature for the RMPC formulation and implementation details.[5,16]

In general, the performance of the SMB separation is optimized in order either to minimize the amount of stationary phase that is used to separate a given amount of feed or to maximize the amount of feed that is separated in a given SMB unit with a fixed amount of stationary phase. Therefore, the productivity (PR), that is, mass of pure product recovered per unit time and unit mass of stationary phase, is one of the key performance parameters to be maximized in the SMB operation.

$$PR = \frac{\text{amount separated per time}}{\text{mass of stationary phase}} = \frac{Q^F c_T^F}{n_{col} V \rho_s (1-\varepsilon)} \qquad (3)$$

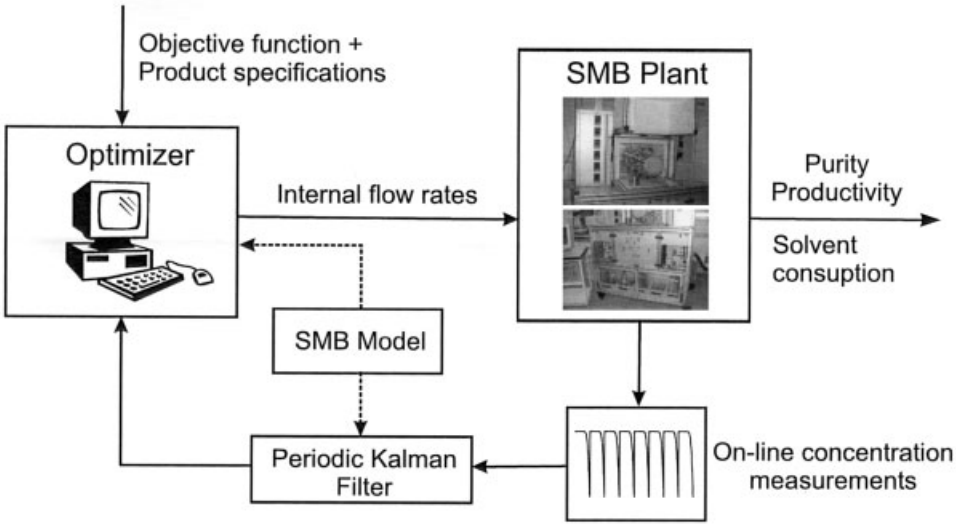

Figure 3. Scheme of the on-line optimization based SMB control concept.

where Q^F is the feed flow rate; c_T^F is the total feed concentration; n_{col} is the number of columns in the SMB loop; V is the column volume; ρ_s is the solid bulk density; and ε is the bed void fraction. Another key performance parameter is the desorbent requirement (DR), which is defined as the mass of desorbent used to recover a unit mass of pure product.

$$DR = \frac{\text{desorbent consumption}}{\text{amount separated}} = \frac{(Q^D + Q^F)\rho_D}{Q^F c_T^F} \tag{4}$$

where Q^D is the desorbent flow rate and ρ_D is its density. Note that the density of the feed stream is assumed to be equal to the solvent density because of its high dilution in typical applications.

It is obvious from Eqs. 3 and 4 that, for a given plant layout (that is, total number of SMB columns and their dimensions and distribution within the sections), feed concentration (c_T^F), and constant switching time (t^*), which is based on pressure drop limitations and column efficiency considerations, the optimization of the SMB separation reduces to the maximization of feed flow rate, minimization of the desorbent consumption, or a combination thereof.

Since the primary objective of the operation is the delivery of products with the required specifications, the above economic objective is subject to constraints on the product purities. These can be imposed by constraining the average purities with a lower bound, such as in our case over the prediction horizon of 2 cycles:

$$P_E^{ave} \geq P_E^{min} - s_E \tag{5}$$

$$P_R^{ave} \geq P_R^{min} - s_R \tag{6}$$

$$s_i \geq 0 \quad (i = E, R) \tag{7}$$

Note that raffinate and extract purities can be calculated directly from the model outputs (Eqs. 1 and 2) and the corresponding outlet flow rates, that is, $Q^E = Q_I - Q_{II}$ and $Q^R = Q_{III} - Q_{IV}$. Since the average purity expressions are nonlinear in terms of flow rates and output concentrations, they are successively linearized and included in the optimization problem as linear inequality constraints. The stipulated purity constraints may render the optimization problem infeasible, for instance, during the startup phase of the operation or because of a disturbance at a particular time step. Therefore, it is common practice to introduce slack variables, that is, s_E and s_R, which are kept small by introducing a penalty term in the objective function (see Eq. 13).

Similar to product purities, the constraints due to hardware limitations can also be enforced as constraints of the optimization problem as follows:

$$0 \leq Q_j \leq Q^{max} \quad \text{for} \quad j = I, \ldots, IV \tag{8}$$

$$|\Delta Q_j| \leq \Delta Q_j^{max} \quad \text{for} \quad j = I, \ldots, IV \tag{9}$$

Here, Eq. 8 is to make sure that the pressure drop in the columns is kept below a certain maximum level at all times, whereas Eq. 9 restrains the maximum allowable internal flow rate changes in order to avoid sudden large pressure changes in the SMB columns. For the physical consistency of the problem, the predicted output concentration values must be nonnegative:

$$\mathbf{c}_{out}^{n_p} \geq \mathbf{0} - \mathbf{s} \tag{10}$$

$$\mathbf{s} \geq \mathbf{0} \tag{11}$$

where $\mathbf{0} := [0 \ldots 0]^T$ with proper dimensions. Also, the external flow rates have to be positive:

$$0 \leq Q_{external} \tag{12}$$

The objective function completes the optimization problem. Here, the objective is that of minimizing the cumulative solvent consumption and maximizing the cumulative throughput over

the prediction horizon, that is, $nc = 1$ cycle. This can be formulated in terms of minimization of the following function:

$$\min_{\mathbf{Q}^{n_c},\mathbf{s}} [\lambda_D Q_D^{n_c} - \lambda_F Q_F^{n_c} + \lambda_E s_E + \lambda_R s_R + \boldsymbol{\lambda}_s \mathbf{s}] \qquad (13)$$

In the equation above, $Q_D^{n_c}$ and $Q_F^{n_c}$ are the cumulative solvent consumption and throughput over the control horizon, respectively; $\mathbf{Q}^{n_c}$ comprises the manipulated variables, that is, internal flow rates, for the whole control horizon; λ_D and λ_F are the weights of desorbent consumption and throughput terms, respectively; λ_E, λ_R, and $\boldsymbol{\lambda}_s$ are the weights of the corresponding slack variables, which are kept large in order to punish their unnecessary use. The minimization (Eq. 13) together with the linear constraints on the input and output values, given by Eqs. 5 to 12, constitute a standard linear programming (LP) problem, for which well-established algorithms and commercial solvers are available. In our work, we use ILOG CPLEX 7.0 as the commercial LP solver. The maximum computation time to solve the LP, i.e., with approximately 3000 constraints and 280 variables, was 1.2 s on a PC with a 3-GHz processor, which is far below any sampling time that one needs for the on-line optimization based control of the SMB process.

Experimental Implementation

This section is devoted to the implementation of the control concept on a laboratory SMB plant. The first goal is to experimentally evaluate and demonstrate the capability of the controller to deliver the products with the required specifications by exploiting at the same time the full potential of the SMB process in terms of productivity and solvent consumption. The second goal is to assess the controller performance under uncertainties and disturbances.

To this aim, the control scheme is implemented on a lab-scale SMB unit that consists of eight HPLC columns (10 cm $\times$ 1 cm) distributed as two columns per section (2–2-2–2 configuration). The sectional flow rates of the unit are manipulated by acting on one internal and three external flow rates, that is, Q_I, Q^E, Q^F Q^R, by using four Jasco PU-987 HPLC pumps (see Figure 1). The periodic switching mechanism is implemented by five (12+1) port multi-position valves (Vici-Valco EMT-6-CSD12UW), that is, each associated with one inlet, outlet, or solvent recycle line. The operation of the SMB unit is fully automated by using Laboratory Virtual Instrument Engineering Workbench (LabVIEW, National Instruments). The LabVIEW application is designed such that it acts as an autonomous interface to the on-line control scheme, which is implemented in a MATLAB environment and runs on a separate computer.[24] The unit is located in a climate controlled room for isothermal operation. The technical details of the SMB plant are provided elsewhere.[6,21,25]

As a model application, the SMB unit is used for the high purity separation of the nucleosides uridine and guanosine (Sigma-Aldrich Chemie GmbH, Steinheim, Germany), denoted by U and G, respectively, in the following, on the reversed phase SOURCE^{TM} 30RPC (Amersham Biosciences AB, Uppsala, Sweden). The stationary phase is slurry packed into the HPLC columns by using a solvent mixture of 97% water and 3% ethanol with a flow rate of $Q = 40$ mL/min and 30 min packing time. The average overall void fraction of the columns is found to be $\varepsilon_{ave} = 0.375$ (with a standard deviation of 0.002).[21]

Since the concentration levels in the two outlet streams are the measured variables and constitute the feedback information for the control scheme, two sensors, that is, one at each of the outlets, are needed to monitor the concentration of nucleosides in the product streams continuously. Note that each product stream is a binary mixture; hence, at least two independent signals are required to calculate the concentration levels. Here, we exploit the difference in the UV spectra of uridine and guanosine in order to monitor their on-line concentrations. The absorbance of each product stream is measured by a multi-wavelength UV 2077 (Jasco) detector (see Figure 1) at four different wavelengths simultaneously.[21] The resulting over-determined system of linear equations

$$S_{\lambda_n} = k_{\lambda_n}^U c_U + k_{\lambda_n}^G c_G \quad \lambda_n = \lambda_1, \ldots, \lambda_4 \qquad (14)$$

is solved by a least squares regression, thus improving the measurement accuracy and robustness. In the equation above, $S_{\lambda n}$ is the UV signal at the wavelength λn; $k_{\lambda_n}^U$ and $k_{\lambda_n}^G$ are the calibration factors for uridine and guanosine, respectively; the concentration of uridine c_U and guanosine c_G are the unknowns to be calculated. The accuracy of the on-line monitoring system has been checked by off-line HPLC measurements for a number of SMB experiments and found to be satisfactory, that is, a maximum error of 0.5% is observed.[25]

Before implementing the control algorithm, the retention behavior of the nucleosides has been measured for different solvent compositions (ethanol/water mixture). In all cases the retention behavior can be described by a linear adsorption isotherm:

$$q_i = H_i c_i \quad (i = U, G) \quad \text{where} \quad H_G > H_U \qquad (15)$$

In the above equation, q_i and c_i are the adsorbed phase and liquid phase concentration of component i, respectively; H_i is its Henry's constant. It has also been observed that the higher the ethanol content in the solvent mixture, the lower both the Henry's constants of the nucleosides and the selectivity of the system, that is, $S = H_G/H_U$. Note that higher selectivity implies an easier and more robust separation. On the other hand, lower Henry's constants are preferable because they imply a faster separation. Here, the solvent composition has been chosen to be 5% ethanol and 95% water, as a compromise. The chosen composition is favorable also because it allows operating the SMB columns in an environment similar to their packing conditions, thus minimizing the risk of change in the column characteristics during the operation. The Henry's constants of the nucleosides (at 23°C for 5% ethanol in water) are measured to be $H_U = 1.303$ and $H_G = 2.248$. The details about the system characterization are reported elsewhere.[21]

The design of the SMB separation can be easily done with the help of the triangle theory,[4] which is also used to interpret the control experiments in the following. Therefore, for the sake of completeness, a brief summary of the triangle theory results focusing on the systems characterized by linear isotherms are provided here.[4]

The triangle theory defines the key operating parameters as

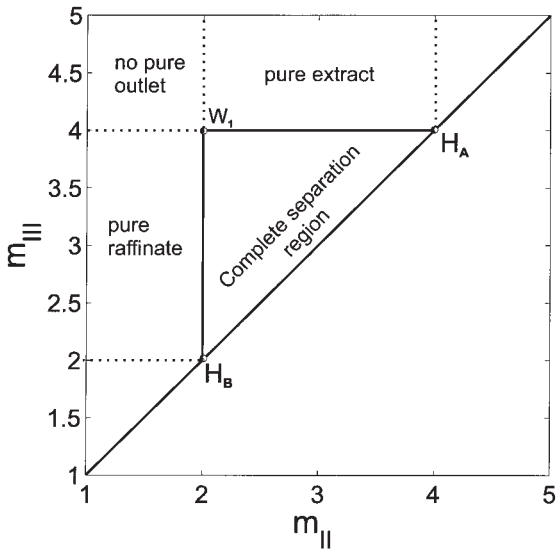

Figure 4. The (m_{II}, m_{III}) operating parameter space for a system characterized by a linear adsorption isotherm.

the ratio of the net fluid and solid phase flow rates in each section of the SMB unit:

$$m_j = \frac{Q_j t^* - V\varepsilon}{V(1-\varepsilon)} \quad (j = I, II, III, IV) \tag{16}$$

and derives the necessary and sufficient conditions on the operating parameters for the complete separation on the basis of the equilibrium theory. Concerning the complete separation of a system characterized by a linear adsorption isotherm (Eq. 15), the conditions for complete separation are as follows:

$$H_G < m_I < \infty \tag{17}$$

$$H_U < m_{II} < m_{III} < H_G \tag{18}$$

$$0 < m_{IV} < H_U \tag{19}$$

under the assumption that nonporous particles constitute the solid phase. Fulfillment of the first condition (Eq. 17) guarantees the regeneration of the solid phase in section I, and its violation leads to poor raffinate purity. Similarly, the constraint on the operating variable m_{IV} (Eq. 19) is necessary for the complete regeneration of the liquid phase in section IV; hence, its violation results in pollution of the extract stream.

The constraints on the operating parameters m_{II} and m_{III} (Eq. 18) guarantee the complete separation of the species in the two central sections; $m_{II} < m_{III}$ is required to have a positive feed flow rate. Provided that the solid and the liquid phases are regenerated completely, the operating parameters m_{II} and m_{III} define a plane, which is divided into several regions. The position of the operating point in the (m_{II}, m_{III}) plane allows predicting the separation performance (see Figure 4). For instance, the operating points within the triangular area defined by Eq. 18 achieve complete separation of the mixture, that is, both the raffinate and extract outlets are pure.

Note that the performance parameters, namely, the productivity (PR) and desorbent requirement (DR) given by Eqs. 3 and 4, respectively, can be expressed in terms of flow rate ratios m_j as follows:

$$PR = \frac{(m_{III} - m_{II})c_T^F}{n_{col} t^* \rho_s} \tag{20}$$

$$DR = \frac{\rho_D}{c_T^F}\left(1 + \frac{m_I - m_{IV}}{m_{III} - m_{II}}\right) \tag{21}$$

It is obvious from Eqs. 20 and 21 that the operating performance of the SMB unit improves by increasing the difference ($m_{III} - m_{II}$). This implies that the optimal operating conditions in terms of solvent consumption and productivity per unit mass of the stationary phase correspond to the vertex of the triangular complete separation region, that is, indicated as W_1 in Figure 4.

Experimental Results

The LTV SMB model (Eqs. 1 and 2) used in the control scheme is obtained as described before using the isotherm information obtained by single column Henry's constants measurements at 23°C, namely, $H_U = 1.303$, $H_G = 2.248$ (henceforth shown by the triangle with solid boundaries), and $\varepsilon_{ave} = 0.375$. These are different from those obtained by running SMB experiments, that is, $H_U = 1.316$, $H_G = 2.140$, and $\varepsilon_{ave} = 0.375$ (henceforth shown by the triangle with broken boundaries). This is done on purpose because such an uncertainty is clearly part of the errors in model parameters typically encountered in applications, as experienced in our case, and the controller should be able to cope with them. The details of obtaining actual isotherm parameters and column characteristics may be found elsewhere.[21] For all experiments below, the switching time is $t^* = 120$ s. One can see from Eq. 20 that the lower the switching time, the higher the productivity. It is also obvious from Eq. 16 that the lower the switching time, the higher the internal flow rates, that is, the switching time is lower bounded by the maximum pressure drop in the unit.

The control problem is formulated such that the performance of the SMB unit is optimized over 2 cycles and the on-line solution of the optimization problem yields the optimal flow rate sequence for the next 1 cycle, that is, the prediction and control horizons are defined as $n_p = 2$ cycles and $n_c = 1$ cycle, respectively. The weights of the desorbent consumption, feed flow, and slack variables in the cost function (Eq. 13) are chosen as $\lambda_D = 2$, $\lambda_F = 10$, and $\lambda_E = \lambda_R = 150$, respectively. This means that the primary task of the controller is to maintain the product purities. Once the product specifications are fulfilled, the maximization of the throughput has priority while the reduction of the solvent consumption is of secondary importance. Table 2 gives the parameters used for the synthesis of the controller. Note that since the number of sampling times within a complete cycle is defined to be $N = 64$ and $t^* = 120$ s, the control scheme optimizes the process every 15 seconds.

Table 2. The Parameters Used for the Controller Synthesis

Parameter	Value	Parameter	Value
N	64	t^*	120 s
H_U	1.303	H_G	2.248
ε_{ave}	0.375	$m_{j=I\ldots IV}^{ref}$	2.28, 1.26, 2.29, 1.30
n_p	2 cycles	n_c	1 cycle
λ_D	2	λ_F	10
$\lambda_{E,R}$	150	$\boldsymbol{\lambda}_s$	150

The flow rate ratios are defined as $m_j^{ref} = (Q_j^{ref}t^* - V\varepsilon)/(V(1-\varepsilon))$ where Q_j^{ref} are the sectional flow rates that are used to obtain the LTV SMB model.

Experiment 1: operation under disturbances and uncertainties

The first experimental run, shown in Figure 5, is divided into two parts. The first part, that is, from startup to cycle 49, aims to demonstrate that the controller is able to deliver the products with the specified purities and to optimize the process performance despite the uncertainties in the system behavior that are reflected in errors in the estimated isotherm parameters.

To the first aim, the SMB unit is started up without the controller under inappropriate operating conditions, that is, $m_I = 2.28$, $m_{II} = 1.26$, $m_{III} = 2.29$, and $m_{IV} = 1.30$, and run for 8 cycles to show that these conditions indeed result in low product purities. Figure 5 shows the product purities for the entire operation, that is, 38 hours or 142 cycles. One can observe that the startup operating conditions lead to about 88 and 93% purity for extract and raffinate at the end of cycle 8, respectively. This is not only because of the inappropriate choice of the operating point on the (m_{II}, m_{III}) plane (indicated as p_1 in Figure 6a) but also because of the wrong choices of m_I and m_{IV}. Note that the initial value of the extract purity, that is, 90%, is due to the presence of nucleosides in the SMB columns from a previous experiment.

The controller is switched on after cycle 8 to fulfill a specified purity of $P^{min} \geq 99\%$ for both extract and raffinate. It can be seen from Figure 5 that the required product purities are recovered after about 12 cycles following the activation of the controller. The same figure also gives the production cost (F), which is defined according to the cost function of the optimization problem (Eq. 13) but without the contribution of the slack variables, namely:

$$F = \lambda_D Q_D^{ave} - \lambda_F Q_F^{ave} \tag{22}$$

In the equation above, Q_D^{ave} and Q_F^{ave} are the average solvent consumption and throughput over 1 cycle, respectively. Note that once the controller is switched on, it adapts the operating conditions and fulfills the specified product purities at the expense of the production cost. Figure 6a shows the trajectory of the operating point on the (m_{II}, m_{III}) plane. One can see that the location of the steady-state operating conditions corresponding to cycle 49, that is, shown as p_{49} in Figure 6a, is actually very close to the vertex of the triangular region that corresponds to the optimal operating conditions according to triangle theory.[4]

The second part of the run, that is, from cycle 49 to cycle 142, is meant to show the ability of the controller to maintain the product specifications and the process performance despite disturbances occurring during the run. To this aim, a pump disturbance is imposed to the system right after the end of cycle 49, when the pump controlling the flow rate of section I starts to deliver 5% more than the set-value for the remaining part of

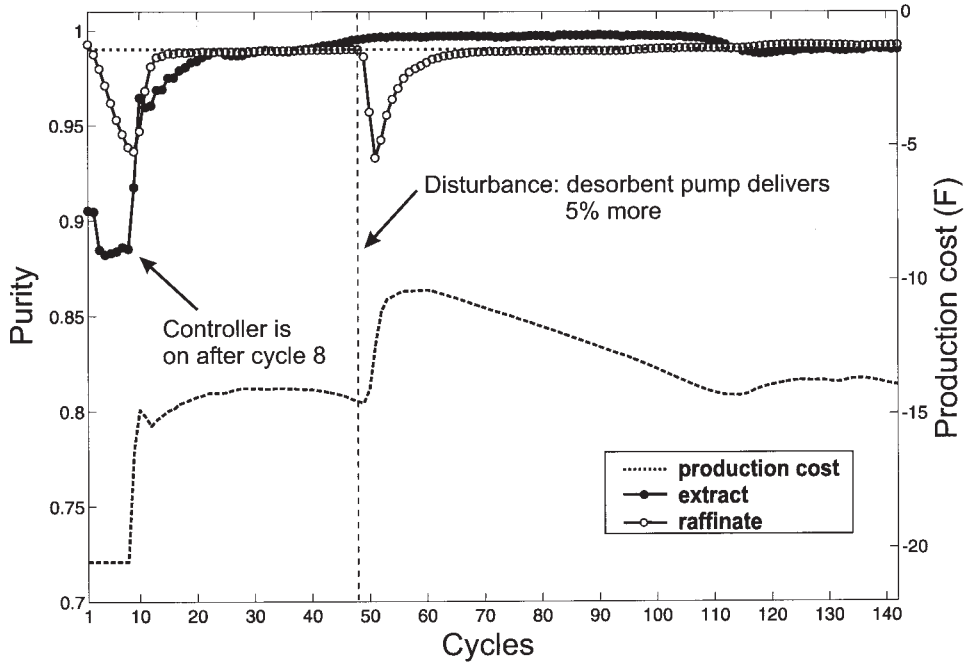

Figure 5. Product purities of extract and raffinate and the production cost (F).

The controller is switched on after cycle 8 in order to achieve a desired purity of above 99% for both products. The disturbance (unknown to the controller) is implemented at the end of cycle 49 by changing the pump calibration factor, and the pump controlling the flow of section I starts to deliver 5% more than it should for the rest of the operation.

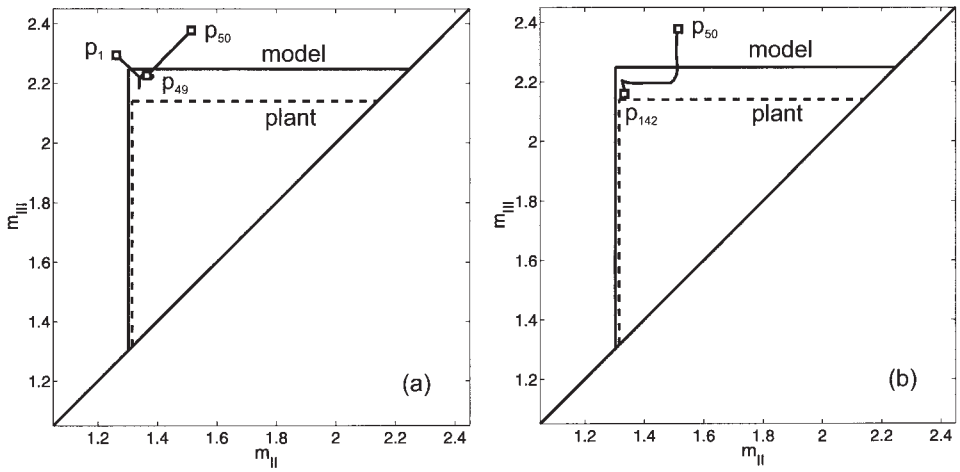

Figure 6. Trajectory of the operating point on the (m_{II}, m_{III}) plane with respect to the region of complete separation.

(a) From the startup to the time just after the disturbance. (b) From the time just after the disturbance to the end of the operation. The regions given by the broken line are applied to the plant at 23°C, whereas the ones with the solid line are based on the isotherm information that is used to obtain the SMB model of the control scheme. p_1, startup operating point. p_{49}, steady-state operating point before the disturbance. p_{50}, operating point just after the disturbance. p_{142}, operating point at cycle 142.

the experiment. This is done by changing the calibration factor of the pump unknown to the controller. Note that this disturbance directly increases all sectional flow rates. A 5% increase in the flow rate of section I leads to approximately 8, 5, and 9% increases in the flow rates of section II, III, and IV, respectively. Figure 7 shows the operating parameters for the whole operation, and the sudden changes in the flow rate ratios due to the disturbance can be clearly observed. Figure 6a illustrates the effect of the disturbance on the operating point in the (m_{II}, m_{III}) operating plane. The conditions immediately before and after the disturbance are indicated as p_{49} and p_{50}, respectively. One can see that the sudden increase in the sectional flow rates moves the operating point to the "pure extract" region and leads to a fast drop in the raffinate purity, which corresponds to the experimental observation in Figure 5. Nevertheless, the controller rejects the disturbance and recovers the product

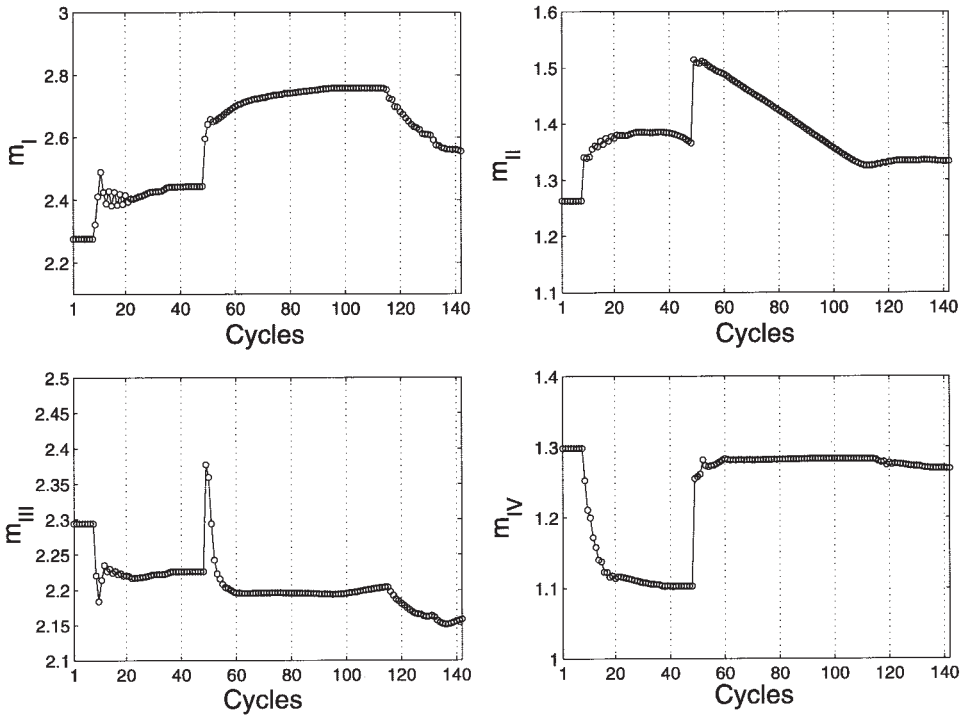

Figure 7. Controller action throughout the operation in terms of flow rate ratios (m_j) that are calculated by average internal flow rates over 1 cycle.

The disturbance on the pump controlling the flow of section I is implemented at the end of cycle 49 and leads to a sudden increase in all m_j values.

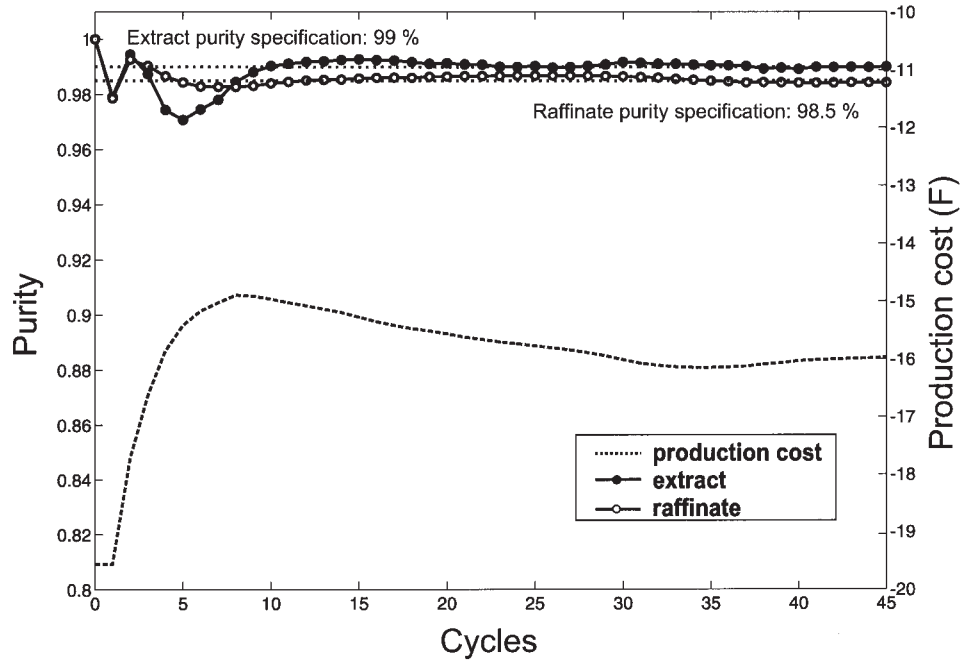

Figure 8. Product purities of extract and raffinate and the production cost (F).

The controller is switched on after cycle 1 in order to achieve a desired purity of above 99% for extract and above 98.5% for raffinate.

purity within 20 cycles, as shown in Figure 5. Figure 6b illustrates the controller action on the (m_{II}, m_{III}) operating plane starting from the time when the disturbance takes place (p_{50}) to the end of the operation (p_{142}). It is seen that the controller drives the operating point first towards the complete separation region in order to fulfill the purity requirements as soon as possible, then the operation performance is optimized by moving the operating point towards the vertex of the triangular area. The evolution of the corresponding production cost is shown in Figure 5.

Variations in the room temperature, such as of $\sim \pm 1$°C, were part of the practice, especially concerning overnight runs.

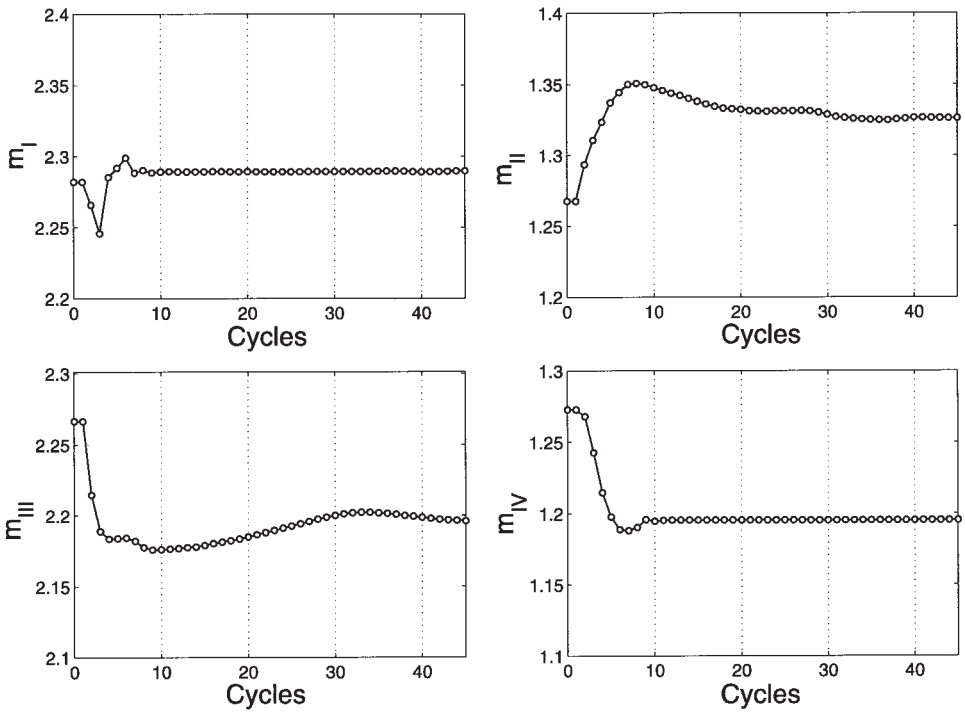

Figure 9. Controller action throughout the operation in terms of flow rate ratios (m_j) that are calculated by average internal flow rates over 1 cycle.

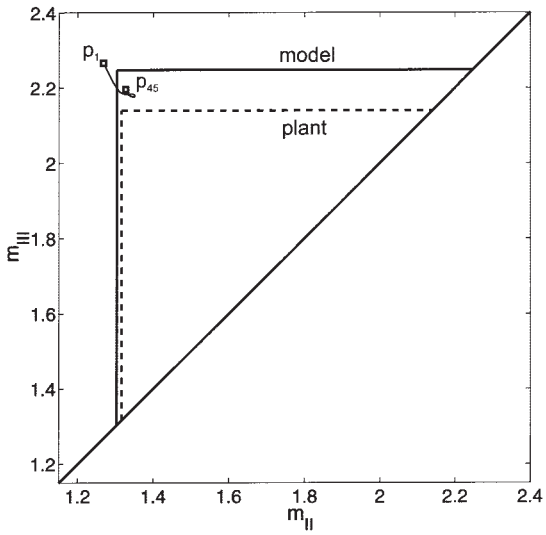

Figure 10. Trajectory of the operating point on the (m_{II}, m_{III}) plane with respect to the region of complete separation.

The regions given by the broken line are applied to the plant at 23°C, whereas the ones with the solid line are based on the isotherm information that is used to obtain the SMB model of the control scheme. p_1, startup operating point. p_{45}, steady-state operating point.

Therefore, deviations in the location of the complete separation region given in Figure 6, which is valid at 23°C, are to be expected since the system is quite sensitive to temperature variation.[21]

Experiment 2: different outlet purity specifications

The previous experimental run addressed high purity separation of nucleosides; thus, the controller was assigned to achieve 99% purity for both raffinate and extract (see Figure 5). On the other hand, in some cases, only one of the species is considered as the product. Accordingly, the second experimental SMB operation addresses a separation in which guanosine is the only target compound to be collected in the extract outlet. The purity requirement of guanosine is specified as $P_E^{min} \geq 99\%$. Note that even if the main interest is in its high purity, the recovery of guanosine in the extract is also important and this requires a certain level of purity in raffinate outlet as well. Therefore, the purity requirement of uridine in the raffinate is specified as $P_R^{min} \geq 98.5\%$.

The SMB plant is started up under the same inappropriate operating conditions as in the previous case (see Figure 5), but here the controller is switched on after the first cycle. Figure 8 gives the outlet purities and the production cost (F) for the whole operation, that is, 12 hours. It can be seen that the specified outlet purities are fulfilled within 10 cycles after the startup. Once the required purities are achieved, the plant performance is optimized and the plant is operated with the minimum production cost after cycle 35. Note that because the product specifications are easier, the achieved production cost is less than the one achieved in the previous experiment (see Figure 5). Figure 9 illustrates the controller action in terms of flow rate ratios (m_j) for the whole operation. The resulting trajectory of the operating point with respect to the region of complete separation in the (m_{II}, m_{III}) plane is given in Figure 10. The startup and the steady-state operating points are indicated as p_1 and p_{45}, respectively.

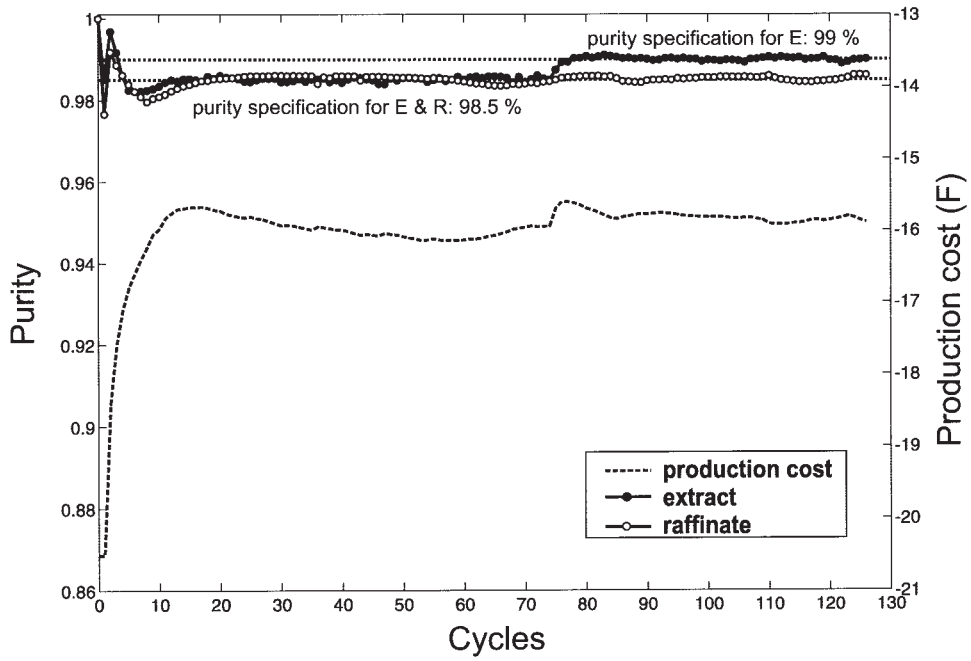

Figure 11. Product purities of extract and raffinate and the production cost (F).

The controller is switched on after cycle 1 in order to achieve a desired purity of above 98.5% for both extract and raffinate. The purity specification of the extract outlet is changed to 99% at cycle 75, whereas the purity specification for the raffinate outlet remains the same, that is, 99%.

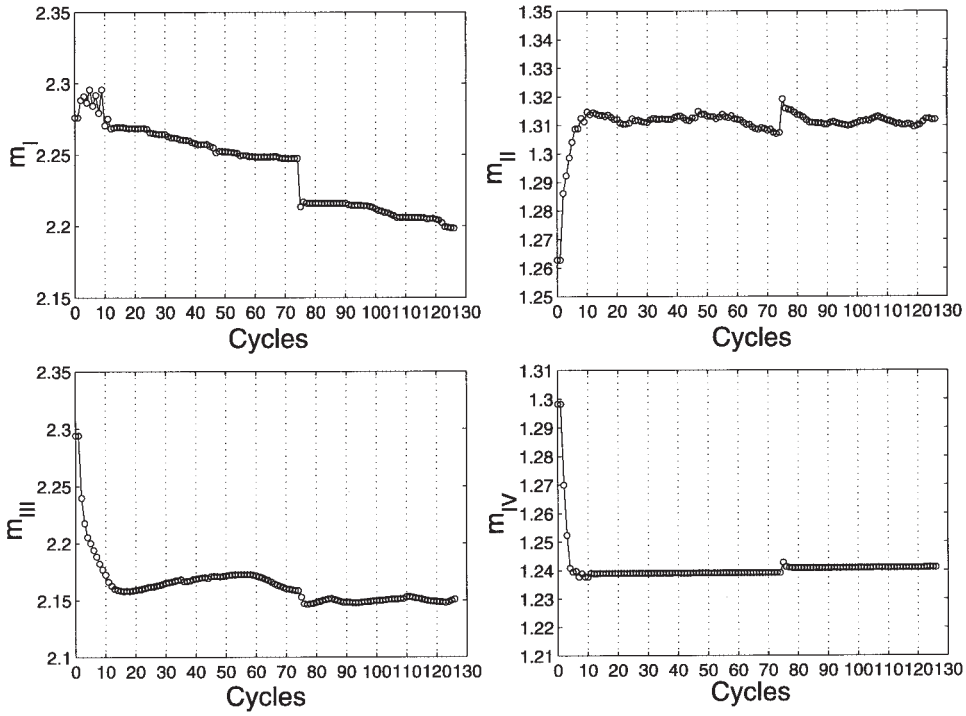

Figure 12. Controller action throughout the operation in terms of flow rate ratios (m_j) that are calculated by average internal flow rates over 1 cycle.

Experiment 3: change in the product purity requirements

The last experimental controlled SMB run is performed to assess the tracking performance of the controller. This scenario addresses a case in which one of the product specifications is changed during the operation.

The SMB unit is started up with the same operating parameters as in the first experiment and the controller is switched on after the first cycle to achieve 98.5% purity for both product outlets. Figure 11 shows the product purities for the entire operation. It can be observed that the specified outlet purities are fulfilled after 19 cycles after the startup and then the operating performance is optimized. The purity specification of the extract outlet is increased from 98.5 to 99% after cycle 74, whereas the purity requirement of the raffinate is kept the same, that is, 98.5%. One can observe from Figure 11 that the controller fulfills the new extract purity requirement within 5 cycles at the expense of the production cost, and it maintains the purity requirement of the raffinate. The controller action in terms of flow rate ratios is given in Figure 12.

Conclusion

Even though SMB has become a state of the art chromatographic separation technology, the robust operation of SMBs at their economic optimum is still an open issue because of the absence of proper process control schemes. The previously proposed SMB control concepts required the availability of accurate physicochemical data and the precise representation of the process dynamics.

Recently, we have introduced an SMB control concept that is based on the on-line dynamic optimization of the process. The effectiveness of the controller has been demonstrated previously when applied to a virtual SMB plant in the case of systems characterized by both linear and nonlinear isotherms.[5,18-20] The performance has been tested thoroughly under extreme model/plant mismatch conditions and disturbances of various origins.[21]

In this work, we address the experimental implementation of the controller to a laboratory eight-column four-section SMB plant, which is used for the separation of uridine and guanosine. The experimental runs are designed to challenge the robust performance of the controller. The results have shown that the controller can minimize the off-spec production, assure the product quality, and optimize the performance of the plant in terms of maximum throughput and minimum desorbent requirement despite uncertainties in the system behavior and major disturbances in the SMB.

Notation

A, B, C = state space model matrices
c_i = concentration of species i [g/L]
F = production cost function [mL/min]
H_i = Henry's constant of species i
k_λ = UV calibration factor [AU l/g]
m_j = flow rate ratio in section j
N = number of time steps per cycle
n_c = control horizon [cycles]
n_{col} = number of columns constituting the SMB unit
n_{eq} = number of equations
n_p = prediction horizon [cycles]
n_u = number of process inputs
n_y = number of process outputs
P = purity
q_i = adsorbed phase concentration of species i [g/L]

Q_j = volumetric fluid flow rate in section j [mL/min]
S = UV signal [AU]
s = slack variable
t^* = switch time [s]
u = input vector of superficial velocities
V = column volume [mL]
x = state vector
y = output concentration vector

Greek letters

ε = void fraction
$\lambda_D, \lambda_F, \lambda_E, \lambda_R, \lambda_S$ = weighting factor in cost function
λ_n = wave length [nm]
ρ = density [kg/m^3]

Subscripts and superscripts

A, B = components
ave = average
D = desorbent
E = extract
F = feed
G = guanosine
i = component index
j = section index ($j = 1..4$)
k = cycle index
max = maximum
min = minimum
n = time step index within a cycle ($n = 0..N - 1$)
n_c = over the control horizon
n_p = over the prediction horizon
R = raffinate
ref = reference
s = solid phase
U = uridine

Literature Cited

1. Ruthven DM, Ching CB. Counter current and simulated counter current adsorption separation processes. *Chem Eng Sci.* 1989;44:1011-1038.
2. Zhang Z, Mazzotti M, Morbidelli M. Multiobjective optimization of simulated moving bed and VARICOL processes using a genetic algorithm. *J Chromatography A.* 2003;989:95-108.
3. Toumi A, Engell S, Ludemann-Hombourger O, Nicoud RM, Bailly M. Optimization of simulated moving bed and Varicol processes. *J Chromatography A.* 2003;1006:15-31.
4. Mazzotti M, Storti G, Morbidelli M. Optimal operation of simulated moving bed units for nonlinear chromatographic separations. *J Chromatography A.* 1997;769:3-24.
5. Erdem G, Abel S, Morari M, Mazzotti M, Morbidelli M, Lee JH. Automatic control of simulated moving beds. *Ind Eng Chem Research.* 2004;43:405-421.
6. Erdem G. *On-line optimization and control of simulated moving bed processes.* Ph.D. Thesis, ETH Zurich, Switzerland; 2005.
7. Kloppenburg E, Gilles ED. Automatic control of the simulated moving bed process for C_8 aromatics separation using asymptotically exact input/output-linearization. *J Process Control.* 1999;9:41-50.
8. Song IH, Rhee HK, Mazzotti M. Identification and predictive control of simulated moving bed process. Proc 3rd Pacific Basin Conference on Adsorption Science and Technology, Kyongju, Korea, 2003.
9. Schramm H, Grüner S, Kienle A. Optimal operation of simulated moving bed chromatographic processes by means of simple feedback control. *J Chromatography A.* 2003;1006:3-13.
10. Klatt KU, Hanisch F, Dünnebier G, Engell S. Model-based optimization and control of chromatographic processes. *Computers Chem Eng.* 2000;24:1119-1126.
11. Klatt KU, Hanisch F, Dünnebier G. Model-based control of a simulated moving bed chromatographic process for the separation of fructose and glucose. *J Process Control.* 2002;12:203-219.
12. Wang C, Klatt KU. Dünnebier G, Engell S, Hanisch F. Neural network-based identification of SMB chromatographic processes. *Control Eng Practice.* 2003;11:949-959.
13. Wang C, Engell S, Hanisch F. Neural network-based identification and MPC control of SMB chromatography. 15th IFAC World Congress, Barcelona, Spain, 2002.
14. Toumi A, Engell S. Optimization-based control of a reactive simulated moving bed process for glucose isomerization. *Chem Eng Sci.* 2004; 59:3777-3792.
15. Engell S, Toumi A. Optimisation and control of chromatography. *Computers Chem Eng.* 2005;29:1243-1252.
16. Lee JH, Natarajan S, Lee KS. A model-based predictive control approach to repetitive control of continuous processes with periodic operations. *J Process Control.* 2001;11:195-207.
17. Natarajan S, Lee JH. Repetitive model predictive control applied to a simulated moving bed chromatography system. *Computers Chem Eng.* 2000;24:1127-1133.
18. Erdem G, Abel S, Morari M, Mazzotti M, Morbidelli M. Automatic control of simulated moving beds—II: Nonlinear isotherm. *Ind Eng Chem Research.* 2004;43:3895-3907.
19. Abel S, Erdem G, Mazzotti M, Morari M, Morbidelli M. Optimizing control of simulated moving beds—Linear isotherm. *J Chromatography A.* 2004;1033:229-239.
20. Erdem G, Abel S, Morari M, Mazzotti M, Morbidelli M. Online optimization based feedback control of simulated moving bed chromatographic units. *Chem Biochem Eng Quarterly.* 2004;18:319-328.
21. Abel S, Erdem G, Amanullah M, Morari M, Mazzotti M, Morbidelli M. Optimizing control of simulated moving beds—Experimental implementation. *J Chromatography A.* 2005;1092:2-16.
22. Morari M, Lee JH. Model predictive control: past, present and future. *Computers Chem Eng.* 1999;23:667-682.
23. Kalman RE. A new approach to linear filtering and prediction problems *Trans ASME, J Basic Eng.* 1960;82:35-45.
24. Lawrence M, Erdem G, Abel S, et al. Online optimization and feedback control of an SMB plant: a LabVIEW Matlab procedural implementation. In: *Proceedings of National Instruments—VIP.* Munich: Germany; 2004.
25. Abel S. *Design and operation of simulated moving bed processes for fine chemical and pharmaceutical separations.* Ph.D. Thesis, ETH Zurich, Switzerland; 2004.

Manuscript received Aug. 16, 2005, and revision received Jan. 23, 2006.